Journal of Additive Manufacturing Technologies
DOI: 10.18416/JAMTECH.2212692

Infinite Science | Publishing

Effects of design parameters on surface roughness of additively manufactured thin-walled structures

V. Yogurtcuoglu[1,2], U. Simsek[1], and B. Koc[2*]

[1]General Electric Aviation, Kocaeli, Turkey
[2]Faculty of Engineering and Natural Sciences, Sabanci University, Istanbul, Turkey
[*] Corresponding author, email: bahattinkoc@sabanciuniv.edu

Abstract

Additive manufacturing (AM) has enabled the production of complex geometries that are not possible to be manufactured through traditional subtractive methods. Among the AM technologies, laser powder bed fusion (LPBF) process has gained considerable attention in many engineering industries due to its capability to fabricate complex parts with intricate details. Especially, its importance is more evident for complex structures with thin walls in the aviation industry. Moreover, many aerospace parts have complex internal channels with thin walls, which may not be accessible for secondary machining operations and hence they must be additively manufactured as-built. Therefore, the surface roughness of additively manufactured thin-wall structures is thoroughly depended on the AM process used. The surface roughness of additively manufactured parts could have big influence on the mechanical properties of the end-product. In this study, thin-wall Cobalt-Chrome (CoCr) specimens are fabricated using LPBF and the effects of process parameters such as wall thickness, build angle, and angle of the laser incidence on the surface roughness are investigated. For that purpose, the surface topologies of manufactured specimens are analysed using an optical profilometer and the relationship between the control parameters and standard surface roughness metrics is presented.

Keywords: Surface Roughness, Thin Wall, LPBF, Design for AM, Build Angle, Laser Incidence Angle

1. Introduction

Thanks to advances in the laser powder bed fusion (LPBF) processes, metal additive manufacturing (AM) technologies have gained a great attention from multiple industries such as aviation, automotive, energy, and biomedical. Laser powder bed fusion (LPBF) or also called selective laser melting (SLM) is a powder bed fusion technology enables to manufacture multiple complex parts with intricate details on the same platform simultaneously. LPBF provides numerous advantages by using entire working volume of the machine, reducing manufacturing time and raw material consumption [1, 2]. However, as-built surface quality of parts produced by LPBF technology is completely dependent on design and process parameters. Poor surface quality can affect the tensile and fatigue properties adversely [3, 4]. Recently in the literature, a lot of attention has been given to understand the effects of process and design parameters on the surface quality.

Surface roughness of additively manufactured structures is influenced by a number of factors, including process parameters which could affect the surface quality during the melting and solidification of the metal powders. Many studies investigated the effects of laser power, scan speed, and hatch distance on surface roughness of additively manufactured samples [2, 5, 6]. Eidt et al. [7] presented the influence of processing parameters on the surface roughness of vertical and inclined surfaces and demonstrated the improved surface roughness with increasing contour laser power.

Beside the process parameters, the effects of design parameters such as build angle, build thickness, and laser incidence angle are also presented in the literature [1, 5, 8]. Yang et al. [5] showed that the surface roughness of inclined surfaces was improved as the build angle increases. In another study, Wan et al. [8] fabricated thin-walled structures in two different thicknesses and reported increasing surface roughness as the build thickness increases.

The effect of laser incidence angle was studied by Sendino et al. [1] and it was demonstrated that the surface roughness of the fabricated specimens increased as the samples were located away from the laser focus location. Rott et al. [9] investigated the influence of build orientation in relation to the laser incidence angle on surface roughness of LPBF parts. A novel “laser relation angle” parameter was introduced to describe the interdependency between surface orientation and laser incidence angle. This parameter was used to describe the position dependent surface roughness.

Even though there is a substantial number of research that concentrated on the relationship between process and design parameters and surface quality, there are only a few that addressed this relationship for thin-walled structures. The main reason is that the fabrication of thin-wall structures is challenging since these structures are more sensitive to distortion due to unconformities in microstructures and melt pool boundaries [10, 11]. For the design and manufacturing of lightweight components, particularly in aerospace applications, the use of thin-walled structures is crucial, and LBPF technology plays an important role in attaining this goal. In several studies, wall thicknesses up to 5 millimetres (0.196 in) considered as thin-walled structures. [10, 11, 16]. For this study, thin wall limit is defined as 0.075 inches considering design and manufacturing constrains.

In this study, the effects of sample thickness, build angle, and angle of laser incidence on the surface roughness of thin-walled structures produced through LPBF process are investigated. For this purpose, a total of 27 thin wall samples are fabricated with varying build angle (50°, 60°, 70°) and sample thickness (0.035″, 0.055″, 0.075″) values with three replicates for each angle-thickness combination. The replicates of the samples are located on different regions of the build platform to capture the effect of the angle of laser incidence.

To measure the up-skin and down-skin surface quality of the printed specimens, the focus variation technique with a surface profilometer, Alicona™ Infinite-Focus G5 instrument is used. The measured surface roughness metrics are analysed using analysis of variance (ANOVA) procedure in Minitab™ software to reveal the influencing parameters and their impacts.

2. Material and methods

2.1. Experimental methodology

This section describes the methodological procedure to characterize the effects of the design and manufacturing parameters on the surface quality of thin-walled structures. The aim is to help the designer to keep the surface roughness and surface quality in a certain range to improve material properties such as elastic modulus, yield strength and UTS. In this study, by means of a Design of Experiment (DoE) and an analysis of Variance (ANOVA) test, the potential influencing variables on the surface roughness are to be quantified and processed. For this purpose, the part thickness, build angle, and distance of the samples from laser origin are used as design variables. The details of the DoE will be discussed in section 2.2.

For manufacturing the samples, Concept Laser M2 machine with a dual-laser configuration was used. All specimens are manufactured by using a single laser to eliminate any variations between lasers. During manufacturing, 50 µm layer thickness, 180 W laser power, 1500 mm/s scanning speed, and 60 µm hatch spacing parameters are utilized under an argon gas environment [17]. Figure 1 shows the position of the used laser and the effect of laser incidence angle on the parts located in different locations [1]. Therefore, the angle of laser incidence is a varying parameter based on the location of the samples with respect to the laser focal point.

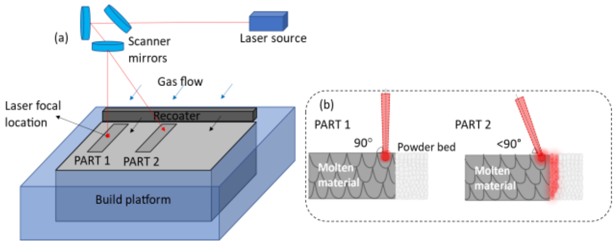

Fig 1. Effect of laser incidence angle: (a) Representation of L-PBF process, (b) Detail of laser incidence angle (Adapted from Sendino et al. [1]).

Fig. 2 shows the build plate with marking of the build direction, recoater direction, and the focal position of the laser. The samples that are included into this study are highlighted with the green colour. The angle of the laser incidence is represented by a factor of the minimum distance between the centre of the gauge section of the specimens and the projected point of the laser focal location onto build platform. In Fig. 2, the red points on the samples indicate the middle points of the gauge sections and the distance to laser origin parameter is represented by letter "D".

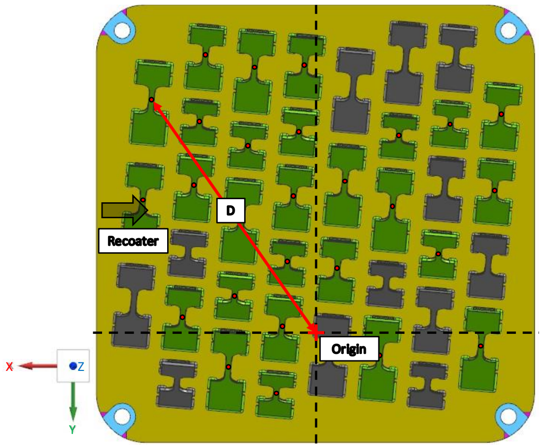

Fig 2. Schematic representation of the specimens on the building platform and laser orientation.

Once the thin-walled specimens are designed and placed on the build plate, considering the manufacturing restrictions, the specimens made of CoCr are fabricated in Concept Laser M2 machine. Fig. 3 shows the fabricated test specimens on the build platform. Three samples which were placed as back-up samples are failed during manufacturing process due to build stop. Since the build stop occurred after the gauge sections were fabricated and three replicates for each coupon designs were successfully manufactured, the statistical analysis was not affected due to the failed samples. After the building process, the specimens are removed from the build platform by Electrical Discharge Machining (EDM). In order to analyse the surface quality, gauge sections of the manufactured specimens are scanned by a focus variation microscope (Alicona).

Journal of Additive Manufacturing Technologies
DOI: 10.18416/JAMTECH.2212692

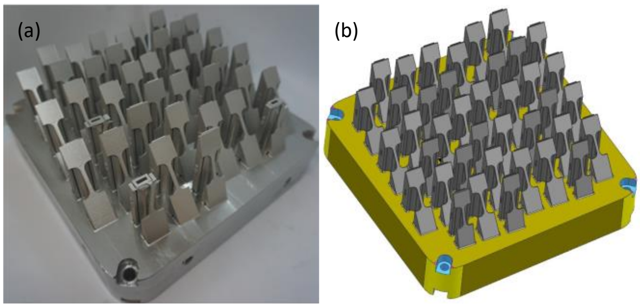

Fig 3. (a) Fabricated test specimens on build platform, (b) CAD model of the build layout.

2.2. Analysis of Variance (ANOVA)

Investigating the effect of the build angle, sample thickness, and distance from laser focus on surface roughness was the ultimate goal of this study. For this purpose, coupons with varying thickness and build angle values were designed and they were placed on build platform with varying distances from the laser focus location. Table 1 summarizes the DoE. Fig. 4 shows the build angles of the fabricated specimens with support structures.

Table 1. Design of experiment.

Variables	Levels		
	-1	0	1
Build orientation (degrees)	50	60	70
Sample thickness (in)	.035	.055	.075
	Interval		
Distance to laser origin (in)	0.696 – 6.540		

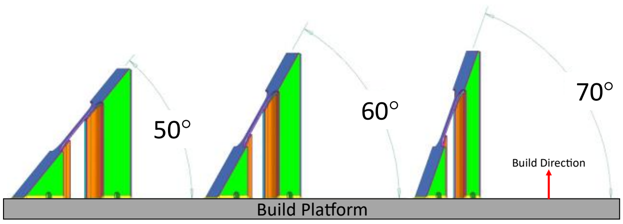

Fig 4. Schematic representation of the build orientations of the specimens; green colour: support structures, blue colour: printed specimens.

ANOVA was performed to quantify the significance of build orientation (O), sample thickness (T), and distance from laser focus (D) on the arithmetical mean height (Sa) for the down-skin and up-skin surfaces of the gauge section. In ANOVA procedure, P-value approach is used to determine the significance of the terms. P-values are compared with the predefined alpha value (α=0.05) and the significance criteria is defined as $P \leq \alpha$ [12].

In the first step of the ANOVA, all linear terms of O, T, and D, all square terms (O*O, T*T, D*D), and two-way interaction terms (O*T, D*T, O*D), are employed to analyse the significance of each term in the measured value of surface roughness. Insignificant terms are eliminated from the regression models step-by-step to converge well fitted models for up-skin and down-skin Sa.

2.3. Surface Roughness Measurement

The surface roughness of the fabricated thin-walled specimens was evaluated with an Alicona™ Infinite-Focus G5 instrument by utilizing focus variation (FV) method. Fig. 5 shows the measurement setup. During the measurements, a 20X objective lens was used and ring light illumination was selected. Lateral and vertical resolutions were determined as 3.51 µm and 12 nm respectively [14].

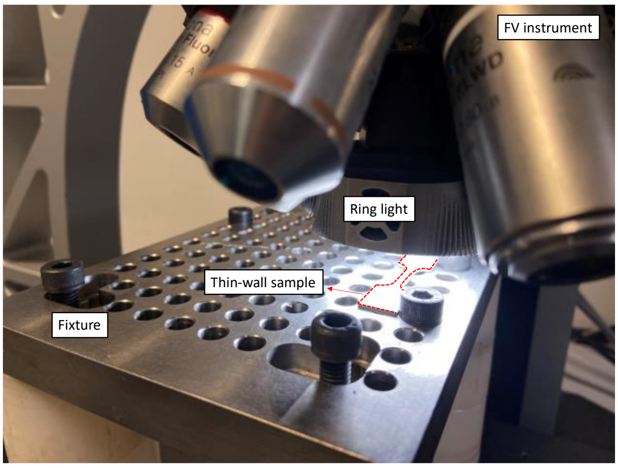

Fig 5. Surface roughness measurement setup.

In Fig. 6, the scanned area of 0.062 in^2 from gauge section is shown in green colour. Gaussian Filter was performed on the 3D-view dataset according to EN ISO 11562 and areal surface roughness metrics are calculated with a cut-off length of 0.13 inches by Alicona™ according to EN ISO 4287. Sa values of the down-skin and up-skin surfaces are reported and analysed in this study. The examples of generated surface topologies are shown in Fig. 7.

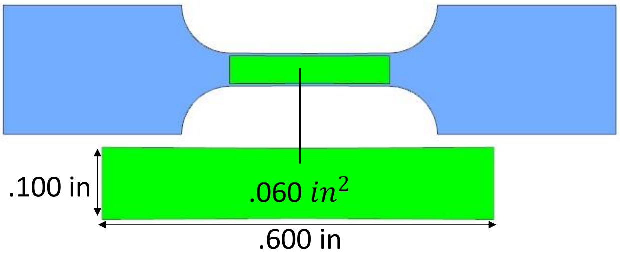

Fig 6. Scanned area of the gauge sections.

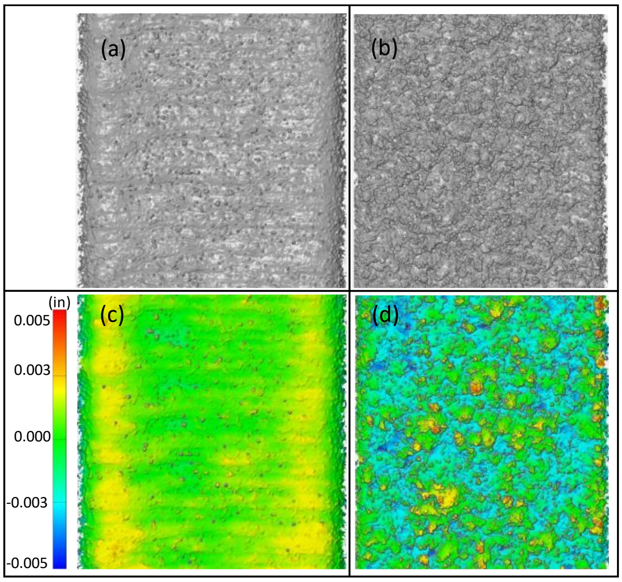

Fig 7. Surface texture produced with Alicona™ Infinite-Focus G5 (a) up-skin, (b) down-skin, (c) up-skin surface height colour plot, (d)down-skin surface height colour plot.

3. Results and discussion

3.1. ANOVA results

The measured areal surface roughness results have been studied to analyse the possible influence of the build orientation, sample thickness, and angle of laser incidence on the surface quality. The sequential assessments have been carried out as defined in Section 2.2. In the regression analysis procedure, outlier data points are eliminated from the model to approach better fitted regression models. Details of the samples included into regression analysis is given in Table 2. A total of 21 data points is used in up-skin and down-skin Sa regression analyses.

Table 2. Measured Sa values for US and DS surfaces.

Sample number	Build orientation (degrees)	Sample thickness (in)	Distance from laser focus (in)	Sa Up-skin (μin)	Sa Down-skin (μin)
22	50	.035	3.381	397.4	1040.0
15	60	.035	5.898	367.4	1031.0
23	60	.035	1.505	316.6	680.0
26	70	.035	4.732	345.9	594.0
10	50	.055	5.957	409.5	1244.0
27	50	.055	3.270	402.9	1077.0
39	50	.055	3.707	368.9	911.3
4	60	.055	6.540	384.8	1034.7
17	60	.055	3.027	353.9	781.6
37	60	.055	5.079	385.4	974.0
11	70	.055	4.364	309.1	525.2
31	70	.055	5.502	386.2	627.8
20	70	.055	1.580	258.5	353.6
1	50	.075	6.237	380.2	1233.6
12	50	.075	2.977	376.5	970.5
29	50	.075	1.557	342.3	851.9
6	60	.075	4.151	335.6	795.6
19	60	.075	0.696	314.9	645.2
13	70	.075	1.903	281.0	404.3
16	70	.075	4.427	335.7	543.1
33	70	.075	3.258	324.5	427.0

The final results of the regression analysis for the down-skin and up-skin are given in the Table 3 and Table 4, respectively. The results indicate that the Sa values of the down-skin surfaces are sensitive to the O^2 and D^2 terms, while the Sa values of up-skin surfaces are sensitive to O and the interaction of O, and D terms based on the previously defined P-value criteria. The sample thickness parameter found out to be insignificant based on the same criteria.

Table 3. Regression for Sa value of down-skin surfaces.

Source	DF	Adj SS	Adj MS	F-Value	P-Value
Regression	2	1408618	704309	310.04	0
$D^2(in^2)$	1	333947	333947	147.01	0
$O^2(deg^2)$	1	992587	992587	436.95	0
Error	18	40890	2272		
Total	20	1449508			

Coefficients

Term	Coef	SE Coef	T-Value	P-Value	VIF
Constant	1441.5	43.5	33.11	0	
$D^2(in^2)$	9.881	0.815	12.12	0	1
$O^2(deg^2)$	-0.2221	0.0106	-20.9	0	1

Model summary

S	R2	R2(adj)	R2(pred)
47.66	97.18%	96.87%	96.27%

With these terms a regression model is proposed for Sa as follows:

$$Sa(\mu in) = 1441.5 + 9.881\ \mathbf{D^2(in^2)} - 0.2221\ \mathbf{O^2(deg^2)} \quad (1)$$

where,
O: Build orientation (degrees), D: Distance to laser focus (in)

Table 4. Regression for Sa value of up-skin surfaces.

Source	DF	Adj SS	Adj MS	F-Value	P-Value
Regression	2	26537	13268.3	37.5	0
O(deg)	1	20066	20066.2	56.71	0
O(deg)*D(in)	1	12908	12908.4	36.48	0
Error	18	6370	353.9		
Total	20	32906			

Coefficients

Term	Coef	SE Coef	T-Value	P-Value	VIF
Constant	529.9	30.5	17.39	0	
O(deg)	-3.913	0.52	-7.53	0	1.07
O(deg)*D(in)	0.247	0.0409	6.04	0	1.07

Model summary

S	R2	R2(adj)	R2(pred)
18.8113	80.64%	78.49%	72.85%

With these terms a regression model is proposed for Sa as follows:

$$Sa(\mu in) = 529.9 - 3.913\ \mathbf{O(deg)} + 0.2470\ \mathbf{O(deg)*D(in)} \quad (2)$$

F-value indicates the significance level of the terms [14]. F values given in Table 3 shows that square terms of both build orientation and distance to laser focus are highly significant in terms of surface roughness of down-skin surfaces. When the F-values of the significant terms compared between up-skin and don-skin models it is observed that the significance levels of the down-skin regression terms are higher.

Table 3 and Table 4 include goodness-of-fit statistics terms S, R^2, R^2(adj), and R^2(pred). S indicates how far the data points fall from the fitted values and it is measured in the unit of the response (µin). In general, lower S value means that the model represents the response better [14].

R^2 and R^2 adjusted values of the regression models for down-skin and up-skin surfaces are used for observing the current status of the established regression model. For down-skin regression model, R^2 value of 97.18% implies that the resultant regression model can explain 97.18% of the variation in the response. High R^2 value means that the model fits well with the data. In general, R^2 value increases as new terms added to the regression model. Therefore, R^2 adjusted is a more convenient criteria to understand if addition of a new term results in more reliable regression model [13]. R^2 adjusted values are used to compare the models with different number of predictors as the insignificant terms are eliminated step-by step. The results showed that the proposed regression model reflects the variability in up-skin Sa values by an adjusted R^2 value of 78.49%.

The predicted R^2 indicates that how well the final regression model fits the response for new observations. Models with high predicted R^2 values represents better fitting for the new observed data [14]. For the final down-skin regression, R^2 predicted value of 96.27% indicates fitness of the proposed prediction model (Table 3). Considering the R^2 predicted value of 72.85% for the up-skin regression (Table 4), the level of fitness for the up-skin regression model is less than the regression model for the down-skin surfaces.

The reason for the lower R^2 predicted and R^2 adjusted values for up-skin Sa regression model could be the lower significance level of the build orientation and distance from laser focus parameters when the F values compared with the down-skin Sa regression model. The presence of overhangs for down-skin faces makes the build angle parameter highly significant for down-skin surface roughness. Due to overhangs, the effect of laser incidence angle also varies between up-skin and down-skin faces [15].

After determining the significant factors with ANOVA for up-skin and down-skin Sa values, the influencing parameters are presented individually in section 3.2 and 3.3 to show the trends for each parameter.

3.2. Effects of Build Angle

As it is concluded from Table 3 and Table 4, the Sa values of both down-skin and up-skin surfaces are thoroughly a function of the build angle and distance from laser focus. Fig. 8 shows the effects of the build angle on the down-skin and up-skin surface roughness, respectively. As it can be observed, higher surface roughness is measured for specimens located with lower build angle with respect to the build platform. The results showed that the surface roughness is dependent on the build orientation of the specimens for both down-skin and up-skin surfaces. A similar trend was also reported in [5].

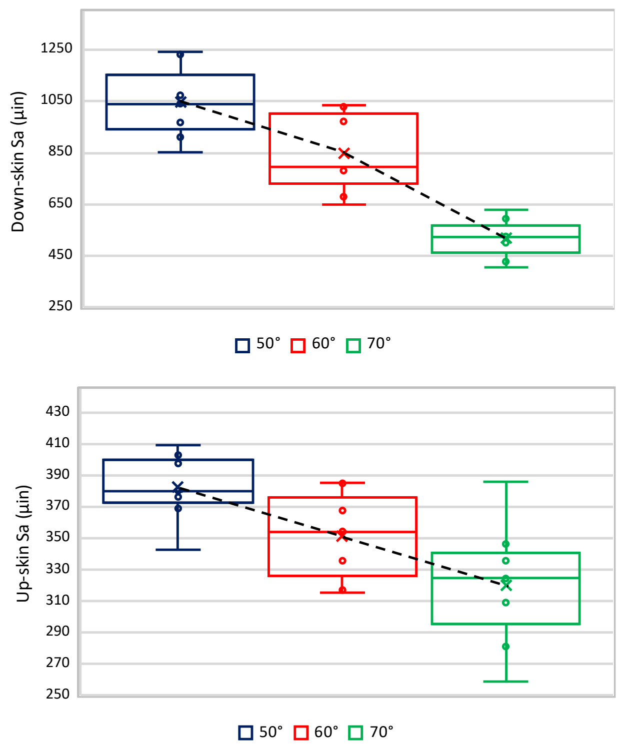

Fig 8. Surface roughness of selective laser melted samples with various degrees of build angle (a) Down-skin surfaces, (b) Up-skin surfaces.

3.3. Effects of Angle of Laser Incidence Angle

Another characterization was carried out to understand the variation of the surface roughness with varying angle of the laser incidence. For this purpose, instead of actual laser incidence angle, the measured distances between the projected location of the laser on the build platform and the mid-points of the gauge sections are taken into consideration for each sample.

Fig. 9 shows the effect of distance to laser focal location, thereby the effect of the angle of incidence, on the surface roughness of down-skin and up-skin surfaces. The results show that even though the specimens were manufactured using the same thickness, build angle and process parameters, the surface roughness is influenced by the position of the specimen on the build plate. As it can be observed in Fig. 9, a higher surface roughness is measured for the specimens located away from the laser. More specifically, for the specimens oriented at 50°, the down-skin surface roughness increases from values of Sa = 851.9 µin for the specimen closest to the laser to Sa = 1244.0 µin for the specimen at the farthest. Similar trends can be observed for the other specimens manufactured with different build orientations [1].

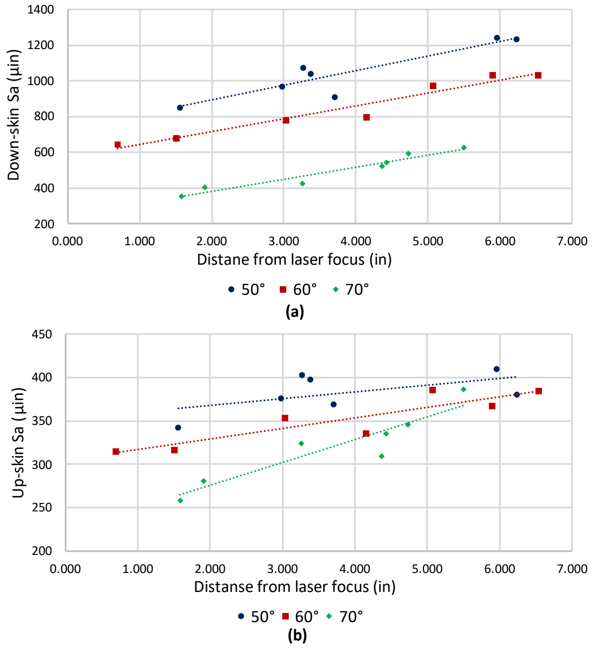

Fig 9. Surface roughness of selective laser melted samples with various distances from laser focus: (a) Down-skin surfaces, (b) Up-skin surfaces.

Due to variation in the angle of laser incidence, the shape of the laser spot gets a non-circular shape at the areas further away from the laser focal location. Consequently, the powder bed is heated differently from the laser focus area and melt pool is not formed in the same way [15]. The effect of this variation is found to be more significant for the down-skin surfaces compared to the up-skin surfaces. For the down-skin surfaces, instabilities at the melt pool regions are suspected to occur due to combination of overhangs and laser incidence angle. These instabilities could cause melt extensions and un-melted particles to stick on the surface [15]. Fig. 10 shows a representation of the incidence angle situation for down-skin and up-skin surfaces.

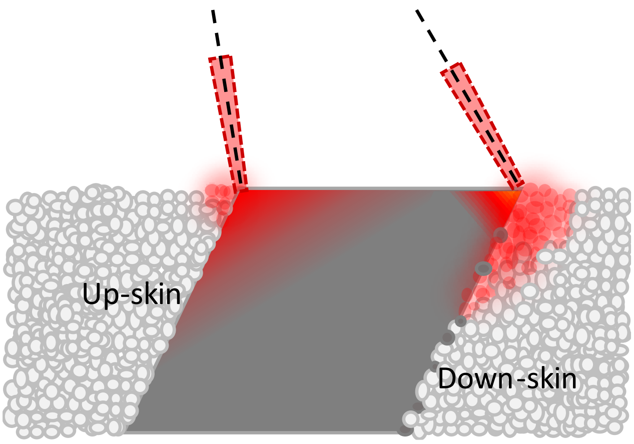

Fig 10. Enlarged schematic representation for up-skin and down-skin surfaces (Adapted from Kleszczynski et al. [15]).

4. Conclusions

This work investigated the effects of the build angle, build thickness, and laser incidence angle on surface roughness of additively manufactured thin-walled CoCr specimens. Laser incidence angle is controlled by varying the sample location on the build platform with respect to laser origin. The findings from the present study are listed below:

1. For up-skin and down-skin surface roughness, the impact of the build angle and the sample location with respect to projected location of the laser onto build platform was found to be significant.

2. It is concluded that the surface roughness increases as the samples were positioned away from the laser origin or as the laser incidence angle increases.

3. The significance level of the distance to laser focus parameter is found to be lower for up-skin Sa compared to down-skin Sa. For down-skin surfaces, instabilities at the melt pool could cause melt extensions and un-melted particles to stick on the surface due to combination of overhangs and laser incidence angle.

4. The surface roughness of the up-skin and down-skin surfaces depends on the build angle. Surface roughness increases as the build angle with respect to build platform decreases.

5. According to ANOVA results, the sample thickness is found to be insignificant. Yet, there are studies that reported the significance of sample thickness in terms of surface roughness. For this study, thickness interval was limited, and the other factors were more dominant. Therefore, a significance for sample thickness was not observed.

The effects of design parameters on surface roughness were demonstrated in this study. The influence of surface roughness on mechanical performance of thin-walled structures can further be investigated. Areal surface roughness metrics are used to characterize the additively manufactured surface topologies. It would be more valuable to identify the most influencing surface roughness metrics on mechanical performance of the fabricated structures. The most critical surface roughness metrics can be determined by optimizing the surface metrology processes. Build and design parameters can be optimized to determine surface roughness metrics and to improve desired mechanical properties of the end-product.

Acknowledgments

This study was carried out under the TUBITAK Technology and Innovation Support Program (grant number: 5158001).

Author's statement

Conflict of interest: Ugur Simsek and Vahap Yoğurtçuoğluis are associated with GE. Informed consent: Informed consent has been obtained from all individuals included in this study. Ethical approval: n/a.

Infinite Science | Publishing

References

1. S. Sendino, M. Gardon, F. Lartategui, S. Martinez, A Lamikiz, *The effect of the laser Incidence angle in the surface of L-PBF processed parts, Coatings*, 2020.10, 1024.
2. E.E. Covarrubias, M. Eshraghi, *Effect of build angle on surface properties of nickel superalloys processed by selective laser melting*, JOM, 2018.70: p. 336–342.
3. J. Gockel, L. Sheridan, B. Koerper and B. Whip, *The influence of additive manufacturing processing parameters on surface roughness and fatigue life*, International Journal of Fatigue, 2019.124: pp.380-388.
4. Everhart, W., Sawyer, E., Neidt, T. et al., *The effect of surface finish on tensile behavior of additively manufactured tensile bars*, Materials Science, 2016.51: p. 3836–3845.
5. T. Yang, T. Dacian, R. Paul, W. *Xinhua, Influences of processing parameters on surface roughness of Hastelloy X produced by selective laser melting, Additive Manufacturing*, 2017.13: p.103-112.
6. C. Amal, E. Ahmed, T. Lore, H. Veit, S. Scholz, *Effect of process parameters on the generated surface roughness of down-facing surfaces in selective laser melting*, Appl. Sci. 2019.9(6), 1256.
7. W. Eidt, E.P. Tatman, J. MCCarther, J. Kastner, S. Gunther, J. Gockel, *Surface Roughness Characterization in Laser Powder Bed Fusion Additive Manufacturing, International Solid Freeform Fabrication Symposium 2019.*
8. H.Y. Wan, Y.W. Luo, B. Zhang, Z.M. Song, L.Y. Wang, Z.J. Zhou, C.P. Li, G.F. Chen, G.P. Zhang, *Effects of surface roughness and build thickness on fatigue properties of selective laser melted Inconel 718 at 650 °C, International Journal of Fatigue*, 2020.137.
9. S. Rott, A. Ladewig, K. Friedberger, J. Casper, M. Full, JH. Schleifenbaum, *Surface Roughness in Laser Powder Bed Fusion – Interdependency of Surface Orientation and Laser Incidence*, Additive Manufacturing 2020.
10. C. Apratim, T. Reza, B. Rasim, M. Waqas, P. Philippe, W. Andrew, Y. Lang, M. Étienne, *In-process failure analysis of thin-wall structures made by laser powder bed fusion additive manufacturing*, Journal of Materials Science & Technology, 2022.98: p.233–243.
11. Y. Tao, X. Deqiao, Y. Wenchao, W. Shuang, R. Peng, S. Lida, Z. Jianfeng, W. Changjiang, *Distortion of thin-walled structure fabricated by selective laser melting based on assumption of constraining force-induced distortion*, Metals, 2019.9(12): p.1281.
12. Montgomery DC. *Design and analysis of experiments*. John Wiley & Sons; 2017.
13. G. Jafar, L. Jianzhi, S. Anil, *Application of optimized laser surface re-melting process on selective laser melted 316L stainless steel inclined parts*, Journal of Manufacturing Processes, 2020.56: p.726–734.
14. N. Lewis, S. Nicola, C. Evangelos, S. Bethan, L. Richard, *Feature-based characterisation of Ti6Al4V electron beam powder bed fusion surfaces fabricated at different surface orientations*, Additive Manufacturing, 2020.35.
15. S. Kleszczyns, A. Ladewig, K. Friedberger, J.Z. Jacobsmühlen, D, Merhof, G. Witt, *Position dependency of surface roughness in parts from laser beam melting systems*, In Proceedings of the 26th International Solid Free Form Fabrication (SFF) Symposium, 2018: p.13–15.
16. X. Lu, M. Chiumenti, M. Cervera, H. Tan, X. Lin, S. Wang, *Warpage Analysis and Control of Thin-Walled Structures Manufactured by Laser Powder Bed Fusion,* Metals, 2021:11, 686.
17. O. Gülcan, U. Simsek, O. Cokgunlu, M. Özdemir, P. Sendur, G.G. Yapici, *Effect of Build Parameters on the Compressive Behavior of Additive Manufactured CoCrMo Lattice Parts Based on Experimental Design*, Metals 2022, 12, 1104.